Biochemical Pharmacology 81 (2011) 510–517

Contents lists available at ScienceDirect

Biochemical Pharmacology

journal homepage: www.elsevier.com/locate/biochempharm

# Methotrexate induces apoptosis through p53/p21-dependent pathway and increases E-cadherin expression through downregulation of HDAC/EZH2

Wen-Yu Huang [a], Pei-Ming Yang [a], Yu-Fan Chang [a], Victor E. Marquez [b], Ching-Chow Chen [a,*]

[a] Department of Pharmacology, College of Medicine, National Taiwan University, Taipei 10018, Taiwan
[b] Laboratory of Medicinal Chemistry, Center for Cancer Research, National Cancer Institute, Frederick, MD 21702-1201, USA

ARTICLE INFO

*Article history:*
Received 1 October 2010
Accepted 22 November 2010
Available online 27 November 2010

*Keywords:*
Methotrexate
p53
p21
HDAC
EZH2

ABSTRACT

Methotrexate (MTX) is a dihydrofolate reductase (DHFR) inhibitor widely used as an anticancer drug in different kinds of human cancers. Here we investigated the anti-tumor mechanism of MTX against non-small cell lung cancer (NSCLC) A549 cells. MTX not only inhibited *in vitro* cell growth via induction of apoptosis, but also inhibited tumor formation in animal xenograft model. RNase protection assay (RPA) and RT-PCR demonstrated its induction of p53 target genes including *DR5*, *p21*, *Puma* and *Noxa*. Moreover, MTX promoted p53 phosphorylation at Ser15 and acetylaion at Lys373/382, which increase its stability and expression. The apoptosis and inhibition of cell viability induced by MTX were dependent on p53 and, partially, on p21. In addition, MTX also increased E-cadherin expression through inhibition of histone deacetylase (HDAC) activity and downregulation of polycomb group protein enhancer of zeste homologue 2 (EZH2). Therefore, the anticancer mechanism of MTX acts through initiation of p53-dependent apoptosis and restoration of E-cadherin expression by downregulation of HDAC/EZH2.



## 1. Introduction

Lung cancer, the major cause of malignancy-related deaths worldwide, has high mortality and poor prognosis due to difficulty of early diagnosis and high potential of invading locally and metastasizing to distant organ [1]. Non-small cell lung cancers (NSCLCs) account for approximately 80% of all lung cancers, and the 5-year overall survival rate is less than 15% [2]. Despite advances in surgery, chemotherapy, and radiotherapy, survival benefits remain poor [3]. Therefore, development of more molecular-targeted therapies is imperative.

The tumor suppressor, p53, functions as a transcriptional regulator in response to stress signals. It is maintained at low level by MDM2 in unstressed cells [4]. However, in response to DNA damage, both quantity and activity of p53 are greatly increased, leading to the expression of p53 target genes including *p21*, *GADD45*, *DR5*, and *Bax* to elicit various responses, such as cell cycle arrest, apoptosis and DNA repair [5]. Post-translational modification (such as phosphorylation, acetylation and ubiquitination) plays a critical role in the regulation of p53 activity and stability. Phosphorylation generally modulates its stability and DNA binding activity [6]. Additionally, p53 is the first non-histone protein acetylated at lysine residues by the acetyltransferases p300 and CBP [7], leading to destabilization of p53-MDM2 interaction and increase of p53-mediated stress response [8].

Overexpression of histone deacetylase (HDAC) and histone-lysine N-methyltransferase EZH2, a catalytic component of polycomb repressive complex 2 (PRC2), have been found in tumors and inhibit the expression of tumor suppressor genes [9–12]. EZH2 could recruit HDAC through EED, another subunit of PRC2, to repress transcription cooperatively [9,10,13]. Therefore, inhibition of HDAC and EZH2 could reactivate tumor suppressive genes and serves as potential anticancer treatments [14–16]. E-cadherin is one of the classic cadherins that mediate cell–cell adhesion at adherens junctions via homophilic binding [17]. Compelling evidences show that E-cadherin is repressed in invasive tumors such as breast, gastric and lung cancers, and its overexpression prevents invasiveness of human carcinoma cells [18,19]. Inhibition of HDACs or EZH2 upregulates E-cadherin and prevents transformation of epithelial cells into metastatic mesenchymal form [20,21].

Methotrexate (MTX), a structural analogue of folic acid and an inhibitor of dihydrofolate reductase (DHFR), is a widely used and highly successful anticancer agent, particularly for human leukemia, severe psoriasis, and some solid tumors [22]. MTX ceases intracellular folate metabolism and finally blocks the synthesis of thymine and purines, leading to impairment of tumor growth and induction of cell death by secondary genotoxic effects

* Corresponding author at: Department of Pharmacology, College of Medicine, National Taiwan University, No. 1, Jen-Ai Road, Section 1, Taipei 10018, Taiwan. Tel.: +886 2 23123456x88321; fax: +886 2 23947833.
*E-mail address:* chingchowchen@ntu.edu.tw (C.-C. Chen).

0006-2952/$ – see front matter © 2010 Elsevier Inc. All rights reserved.
doi:10.1016/j.bcp.2010.11.014

or apoptosis [23]. In the present study, the anti-tumor mechanism of MTX was investigated *in vitro* and *in vivo*. We found that MTX inhibited growth of tumor cells through induction of apoptosis. MTX induced p53 acetylation at Lys373/382 and phosphorylation at Ser15, leading to its stabilization and expression. These effects were correlated with an increase in DNA damage (H2AX phosphorylation) and upregulation of p53 target genes such as p21, DR5, Puma and Noxa. In addition, both MTX and HDAC inhibitor SAHA reduced EZH2 expression. MTX also induced E-cadherin expression as did by EZH2 inhibitor DZNep. These results suggest that MTX initiated p53-dependent apoptosis and suppression of tumor growth, and also induced E-cadherin expression through downregulation of HDAC/EZH2.

## 2. Materials and methods

### 2.1. Materials

The antibodies specific for p53, p21, histone H3 and actin were purchased from Santa Cruz Biotechnology (Santa Cruz, CA). Anti-acetylated p53 (Lys373/382) antibody was from UPSTATE (Billerica, MA). Phospho-H2AX (Ser139) and EZH2 antibody were purchased from Cell Signaling Technology (Danvers, MA). E-cadherin antibody was from Zymed (Carlsbad, CA). Dulbecco's modified Eagle's medium (DMEM), fetal bovine serum (FBS), penicillin, streptomycin, and $TRI_{ZOL}$ were from GibcoBRL (Gaithersburg, MD). Horseradish peroxidase-labeled donkey anti-rabbit second antibody, the ECL detecting reagent, and nylon cellulose membrane were purchased from Amersham Pharmacia Biotech (Uppsala, Sweden). Methotrexate (MTX), propidium iodine (PI), trichostatin (TSA), MS-275, sodium butyrate, oxaflatin, valproic acid (VPA), and 3-(4,5-dimethylthiazol-2-yl)-2,5-diphenyltetrazolium bromide (MTT) were purchased from Sigma (St. Louis, MO). Suberoylanilide hydroxamic acid (SAHA) was kindly provided by Merck (MSD, Taiwan). 3-Deazaneplanocin A (DZNep) was kindly provided by Dr. Victor E. Marquez (National Cancer Institute, MD). Annexin V-FITC Apoptosis Detection Kit Plus was purchased from BioVision (Mountain View, CA).

### 2.2. Cell culture

A549 human lung carcinoma cells from American Type Culture Collection (ATCC) in 2006 were cultured in DMEM. HCT-116 wild-type, p53−/−, and p21−/− cells, kindly provided by Dr. M.W. Van Dyke (M.D. Anderson Cancer Center, Houston, TX) in 2008, were cultured in DMEM. H1299 lung epithelial carcinoma cells from ATCC in 2006 were cultured in RPMI 1640. All mediums were supplemented with 10% FBS, 100 unit/mL penicillin G and 100 mg/mL streptomycin sulfate. Cells were daily checked by morphology and tested to be *Mycoplasma*-free by DAPI staining within the last six months. Gene silencing of HCT116 p53−/− and p21−/− cells was authenticated by ribonuclease protection assay or immunoblot analysis within the last three months.

### 2.3. Preparation of total cell lysates and nuclear extracts

For total cell lysates, cells were lysed in an ice-cold buffer containing 50 mM Tris–HCl, pH 7.4, 150 mM NaCl, 1 mM EGTA, 1% Triton X-100, 1 mM $Na_3VO_4$, 1 mM NaF, 1 mM PMSF, 5 μg/mL leupeptin, and 20 μg/mL aprotinin at 4 °C for 30 min. After centrifugation, the supernatants were transferred to new tubes. For nuclear extracts, cells were resuspended in buffer A (10 mM HEPES, pH 7.9, 10 mM KCl, 0.1 mM EGTA, 1 mM DTT, 0.5 mM PMSF, 1 mM NaF, 1 mM $Na_3VO_4$), then adding 0.6% NP-40. After mixing by vortex for 10 s, the cells were incubated on ice for 15 min. After centrifugation at 5000 rpm for 5 min, the supernatants (cytosolic fractions) were transferred to new tubes. The pellets were lysed in buffer B (20 mM HEPES, pH 7.9, 400 mM NaCl, 1 mM EGTA, 1 mM DTT, 1 mM PMSF, 1 mM NaF, 1 mM $Na_3VO_4$). The suspensions were mixed by vortex for 10 s, followed by sonication in ice-cold water bath for 30 min. After centrifugation at 13,000 rpm for 5 min, the supernatants were used as nuclear extracts.

### 2.4. Western blot analysis

Proteins in the cell lysate (50 μg) are separated on a 7.5–13% SDS-polyacrylamide gel, then transferred electrophoretically onto a nylon cellulose membrane. The membrane is pre-hybridized in 5% skim milk/TBST (20 mM Tris–HCl, pH 7.5, 1.5 M NaCl, 0.05% Tween-20) for 1 h, then transferred to 1% BSA/TBST containing primary antibody and incubated overnight at 4 °C. After washing with the TBST buffer, the membrane is submerged in 1% BSA/TBST containing the horseradish peroxidase conjugated secondary antibody for 1 h. The membrane is washed with TBST buffer, then developed by the ECL system and exposed to X-ray film.

### 2.5. RNase protection assay (RPA)

Total RNA was extracted by $TRI_{ZOL}$ reagent. A RiboQuant Multi-Probe RNase Protection assay (RPA) was performed with the hStress-1, hAPO-3d and hCC-2 biotin-label probe sets (BD Pharmingen, Sparks, MD). The probes were hybridized with 3 μg of RNA, and then samples were digested with RNase to remove single-stranded RNA. Remaining probes were resolved on denaturing 5% polyacrylamide gels.

### 2.6. RT-PCR

Total RNA is isolated by $TRI_{ZOL}$ reagent. Reverse transcription reaction is performed using 2 μg of total RNA and reverse transcribed into cDNA using oligo dT primer, then amplified using two oligonucleotide primers as following: 5′-AGACCGGCGCACAGAGGAAG-3′ and 5′-CTTTTTGGACTTCAGGTGGC-3′ (p53), 5′-CAGAGGAGGCGCCATGTCAG-3′ and 5′-CCTGTGGGCGGATTAGGG-3′ (p21), 5′-GACCTCAACGCACAGTA-3′ and 5′-CTAATTGGGCTCCATCT-3′ (Puma), 5′-AGAGCTGGAAGTCGAGTGT-3′ and 5′-GCACCTTCACATTCCTCTC-3′ (Noxa) or 5′-TGACGGGGTCACCCACACTGTGCCCATCTA-3′ and 5′-CTAGAAGCATTTGCGGGGACGATGGAGGG-3′ (β-actin). PCR is carried out at 94 °C for 30 s, at 55 °C for 30 s and 1 min at 72 °C for 25–35 cycles. The PCR products are subjected to 1–2% agarose gel electrophoresis. Quantitative data are obtained using a computing densitometer and ImageQuant Software (Molecular Dynamics, Sunnyvale, CA).

### 2.7. Cell cycle analysis and Annexin V-FITC staining

Cells were plated in 6-well plates for 24 h, then treated with complete medium containing 50 μM MTX for 24 and 48 h. The floating and adherent cells were harvested and the cell cycle was determined by flow cytometry using a PI stain buffer (5 μg/mL PI and 50 μg/mL RNase A) and analyzed on a BD FACSCalibur cytometer with CellQuest software.

Apoptosis was analyzed by Annexin V-FITC Apoptosis Detection Kit Plus. Briefly, the floating and adherent cells were harvested and resuspended in 0.5 mL of 1× binding buffer containing 5 μL of Annexin V-FITC and 1 μL of SYTOX Green Dye. After incubation at room temperature for 10 min, cells were analyzed by flow cytometry (Ex = 488 nm; Em = 530 nm). The cell population was separated into three populations: live cells with only a low level of fluorescence, apoptotic cells with moderate green fluorescence and necrotic cells with high-intensity green fluorescence.

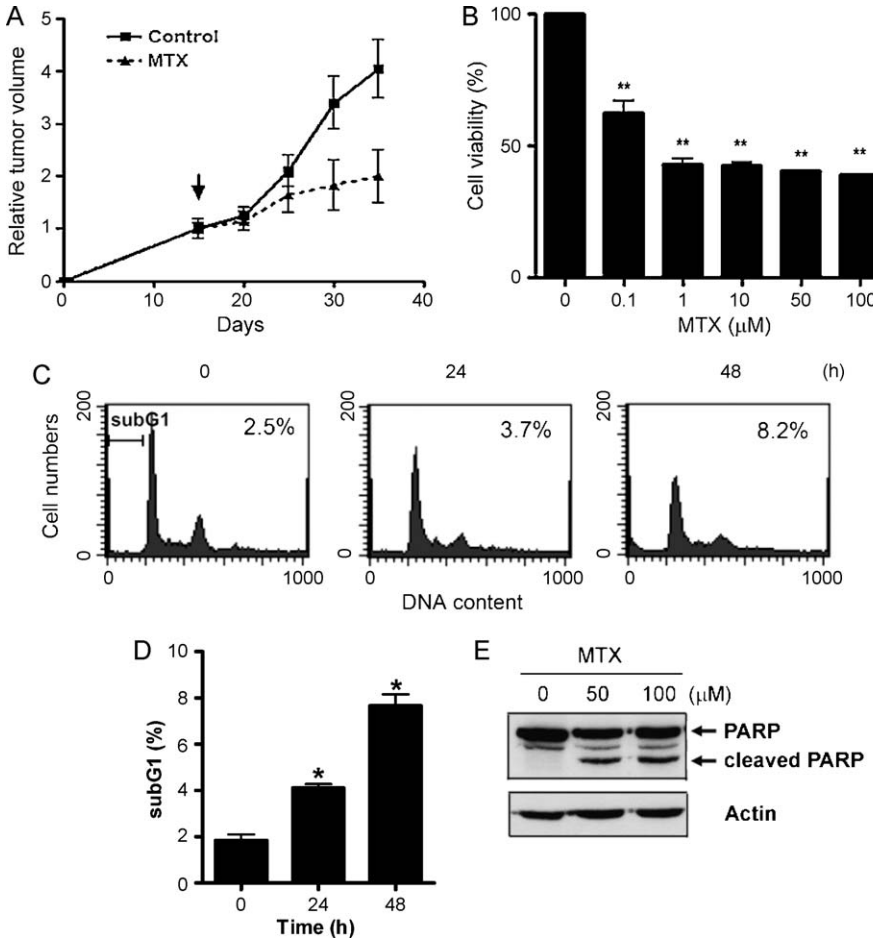


**Fig. 1.** Effects of MTX on cell growth, apoptosis and tumor formation. (A) A549 cells ($10^7$) were xenotransplanted into the right hip region of nude mice. After visible tumor formation, mice were randomly divided into two groups for oral treatment with MTX (10 mg/kg/day) or vehicle as described in "Section 2". The arrow indicates the day to administrate MTX. (B) A549 cells were treated with 0.1, 1, 10, 50 or 100 μM for 3 days. MTT assay was performed and absorbance was measured at 550 nm. $^{**}p < 0.05$, compared with basal. (C) A549 cells were treated with 50 μM MTX for 24 or 48 h. Cells were harvested and examined by flow cytometry as described in "Section 2". The percentages of subG1 fraction represented three independent experiments are plotted in (D). (E) Whole cell lysates of A549 cells exposed to 50 or 100 μM MTX for 48 h were harvested and immunoblotted with anti-PARP antibody.

### 2.8. MTT assay

The cell viability after MTX treatment was measured using MTT assay. Cells were plated in triplicate in 96-well plates and treated with increasing concentrations of MTX. After 72 h incubation, 0.5 mg/mL of MTT was added to each well for an additional 4 h. The blue MTT formazan precipitate was then dissolved in 100 μL of DMSO. The absorbance at 550 nm was measured on a multiwell plate reader. Cell viability was expressed as a percentage of control.

### 2.9. Animal xenograft assay

4–6-Week-old female Balb/c nude mice were injected with $10^7$ A549 cells (suspended in 0.1 mL PBS and mixed with 0.1 mL Matrigel) in the rear left flank. Two weeks after administration, 100–200 $mm^3$ tumors were apparent on all mice, then animals were divided into two groups ($n = 6$). One group was orally received MTX (10 mg/kg/day) and the other received vehicle (soy oil). Mice were observed for 35 days, and tumor growth was measured every five days with calipers. All mice were survived during whole experimental period. Tumor volume was calculated using the formula $V(mm^3) = 0.52 \times [ab^2]$, where $a$ is the length and $b$ is the width of the tumor.

### 2.10. Statistical analysis

Data were analyzed using Student's $t$ test. $p$ values $< 0.05$ were considered significant.

## 3. Results

### 3.1. MTX inhibits cell growth and induces apoptosis in A549 cells

MTX has been shown to suppress cell growth through the inhibition of DHFR. To investigate whether MTX inhibits NSCLC tumor growth *in vivo*, A549 cells were introduced into nude mice via subcutaneous administration. Time-dependent increase in tumor formation was seen after injection of A549 cells. The tumor volume was decreased when administrating MTX (Fig. 1A). The *in vitro* cell growth was also decreased in response to MTX treatment for 3 days (Fig. 1B). The effect of MTX to primary mouse embryonic fibroblasts (MEFs) was examined by MTT assay and no toxicity was observed in response to 100 μM MTX treatment (data not shown). To examine whether cell cycle arrest or apoptosis contributes to MTX-induced growth inhibition, A549 cells were treated with 50 μM MTX for 24 and 48 h and the cell cycle distribution was analyzed by flow cytometry. As shown in Fig. 1C and D, MTX induced apoptosis (subG1 fraction) but not cell cycle arrest. The

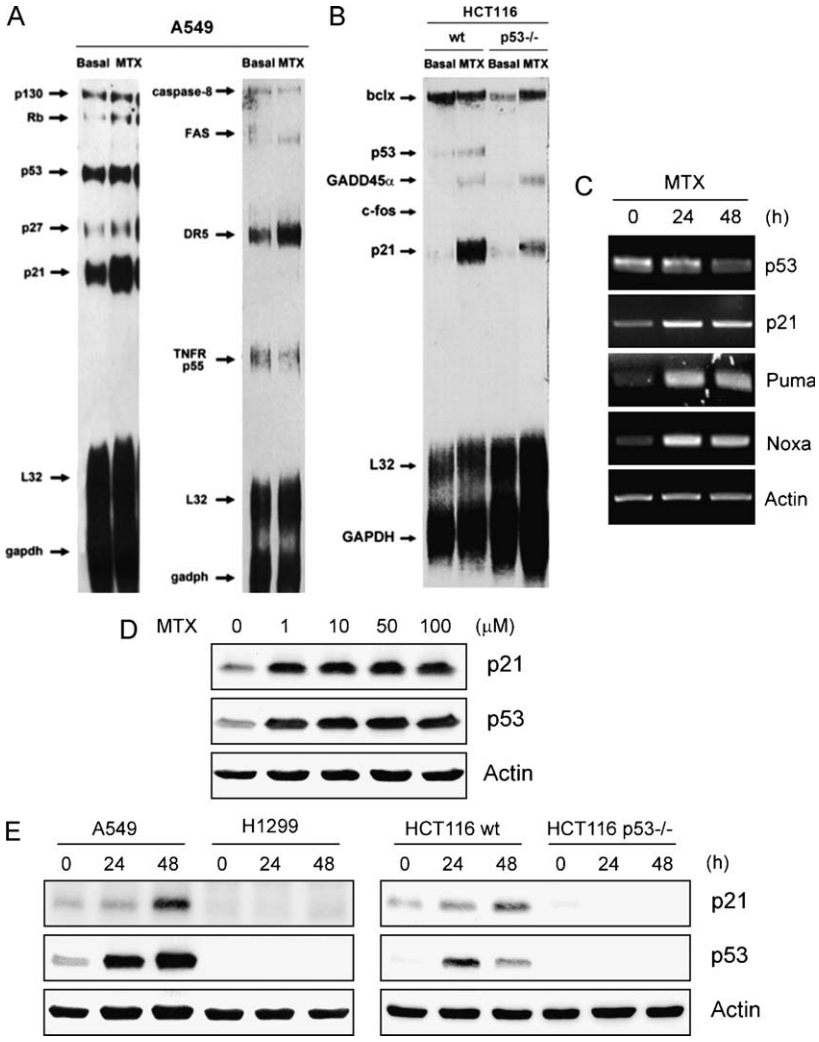


**Fig. 2.** Effect of MTX on p21 expression. Total RNA from (A) A549, (B) HCT116 wild-type (p53+/+), or p53−/− cells treated with 50 μM MTX for 24 h were subjected to RPA as described in "Section 2". GADPH and L32 were shown as internal controls. (C) A549 cells were treated with 50 μM MTX for indicated time intervals. Total RNA were isolated for RT-PCR analysis using primers specific for p53, p21, Puma and Noxa. (D) A549 cells were treated with 0, 1, 10, 50 and 100 μM MTX for 48 h. Whole cell lysates were collected and subjected to western blot with anti-p53 (DO-1) or anti-p21 antibodies. (E) A549, H1299, HCT116 wild-type (WT) and p53−/− cells were treated with 50 μM MTX for 24 and 48 h. Whole cell lysates were collected and subjected to western blot with anti-p53 (DO-1) or anti-p21 antibodies.

apoptotic induction is further confirmed by PARP cleavage (Fig. 1E). These findings revealed that MTX inhibits A549 cell growth via induction of apoptosis.

### 3.2. MTX induces p53-dependent gene expression

To investigate the genes stimulated by MTX, expression of cell cycle- and apoptosis-related genes was examined by RPA. As shown in Fig. 2A and B, MTX increased p21 or DR5 mRNA expression without affecting p53 mRNA in A549 cells and HCT116 cells. However, the induction of p21 mRNA was inhibited in p53−/− cells (Fig. 2B). The mRNA levels of p21 were further evaluated by RT-PCR. As expected, MTX was able to induce p21 but not p53 mRNA expression (Fig. 2C). Moreover, Puma and Noxa, which are critical for the p53-induced apoptotic response [24], were also induced by MTX (Fig. 2C). Time- and dose-dependent increases of p53 and p21 protein by MTX were observed in A549 and HCT116 cells (Fig. 2D and E). To investigate whether MTX-induced p21 expression is dependent on p53, A549 and HCT116 wild-type cells were compared to p53-null H1299 and HCT116 p53−/− cells. MTX-induced p21 expression was abrogated in p53-deficient cells (Fig. 2E). Therefore, these results indicated that MTX induced p53-dependent gene transcription.

### 3.3. MTX induces DNA damage and stabilizes p53 by increasing its phosphorylation and acetylation

DNA damage might be required for MTX-induced expression of p53. As shown in Fig. 3A, MTX caused DNA damage as indicated by the increase of H2AX phosphorylation (γ-H2AX). Post-translational modification of p53 such as phosphorylation and acetylation in response to DNA damage is closely related to its stability and transcriptional activity. MTX induced p53 phosphorylation at Ser15/Ser392 and acetylation at Lys373/382 in nucleus and total cell lysates (TCL), which were coincident with its increase in protein level (Fig. 3B, left and right panels, lanes 1 and 2). To further confirm that MTX induced post-translational modification of p53, proteasome inhibitor MG132 was treated to increase the basal level of p53 (Fig. 3B, right panel, lane 3). In this condition, phosphorylation at Ser15 and acetylation at Lys373/382 were not seen (Fig. 3B, right panel, lane 3), indicating that these post-translational modifications were indeed modified by MTX but not due to an increase of p53 *per se* (Fig. 3B, right panel, lane 4). However, increase in Ser392 phosphorylation was paralleled with the increase of p53 protein. To explore whether MTX modulates p53 turnover, its degradation rate was examined. After treatment with MTX for 24 h, cells were treated with cycloheximide (CHX) for the indicated time. The degradation of

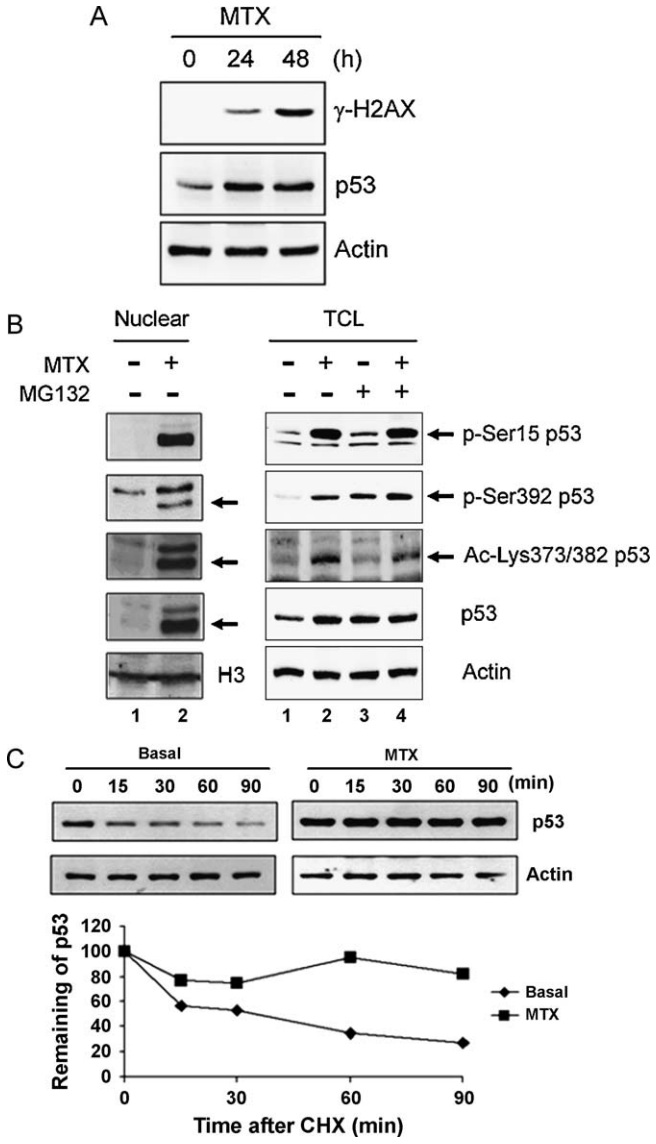


**Fig. 3.** Effect of MTX on post-translational modifications and stability of p53. (A) A549 cells were exposed to 50 μM MTX as indicated time points and total cell lysates were immunoblotted with anti-γ-H2AX or anti-p53 (DO-1) antibodies. (B) A549 cells were treated with 50 μM MTX for 24 h and 50 μM MG132 was added 2 h before cell harvest. Nuclear extracts and total cell lysates were prepared as described in "Section 2." Both kinds of cell extracts were immunoblotted with anti-acetyl-p53 (Lys373/382), anti-phospho-p53 (Ser392), anti-phospho-p53 (Ser15), or anti-p53 (DO-1) antibodies. (C) A549 cells pre-treated with 50 μM MTX for 24 h were exposed to 10 μg/mL cyclohexamide (CHX), and then harvested at different time points as indicated. Total cell lysates were immunoblotted with anti-p53 (DO-1) antibody. p53 expression normalized with actin was quantified using ImageQuant and the p53 remaining is indicated graphically.

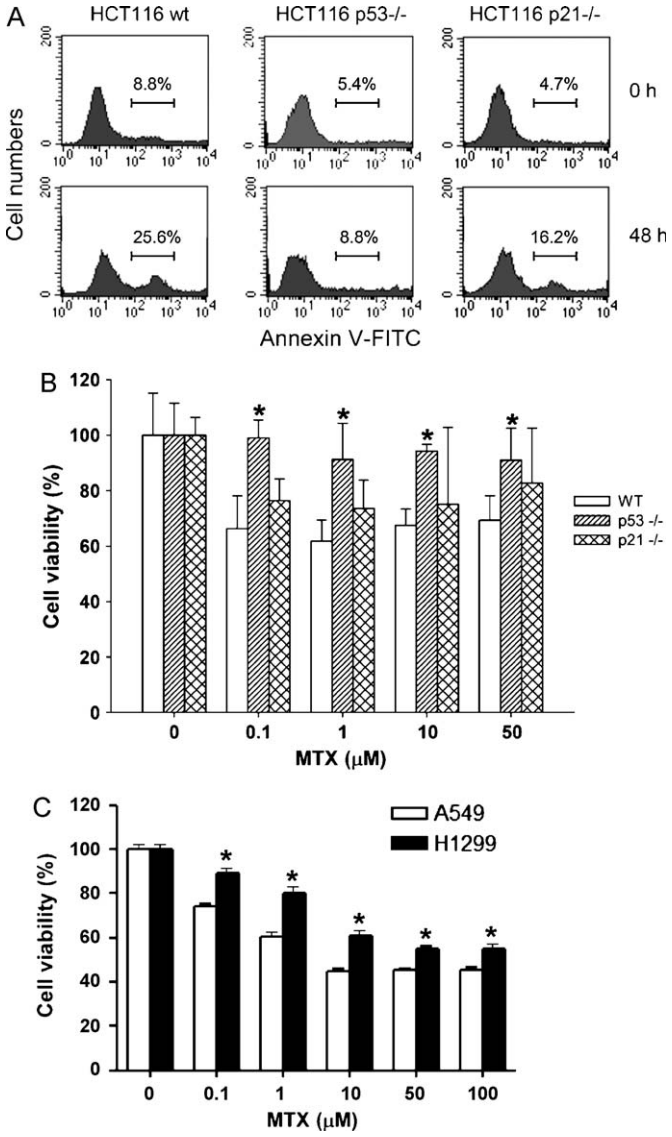


**Fig. 4.** Effect of p53 and p21 on MTX-induced apoptosis and growth inhibition. (A) HCT116 wild-type (wt), p53−/− and p21−/− cells were treated with 50 μM MTX for 48 h. Cells were harvested and examined by Annexin V-FITC staining as described in "Section 2". The percentage of Annexin-FITC positive fraction represented three independent experiments. (B) HCT116 wild-type (WT), p53−/− and p21−/− cells were treated with 0.1, 1, 10 or 50 μM for 3 days. MTT assay was performed and absorbance was measured at 550 nm. $^*p < 0.05$, compared with wild-type cells. (C) A549 and H1299 cells were treated with 0.1, 1, 10, 50 or 100 μM for 3 days. MTT assay was performed and absorbance was measured at 550 nm. $^*p < 0.05$, compared with A549 cells.

p53 was greatly reduced in the presence of MTX, indicating that MTX stabilized p53 by reducing its degradation (Fig. 3C).

### 3.4. MTX induces p53/p21-dependent apoptosis

To investigate the role of p53 and p21 in MTX-induced apoptosis, HCT116 wild-type, p53 or p21 deficient cells treated with 50 μM MTX for 48 h were examined by Annexin V-FITC staining. MTX increased the Annexin V-FITC-positive cells in HCT116 wild-type cells (from 8.8% to 25.6%), which was completely blocked in p53−/− cells (8.8%). Apoptotic induction was partially rescued in p21−/− cells (16.2%) (Fig. 4A). To further examine whether the inhibition of cell growth by MTX is dependent on p53/p21 pathway, HCT116 wild-type, p53−/− and p21−/− cells treated with MTX was performed by MTT assay. Compared with wild-type cells, cells deficient in p53 were resistant to growth arrest induced by MTX (Fig. 4B). However, MTX still induced cell growth arrest in p21−/− cells, suggesting that blockade of p21 pathway alone could not rescue cells from MTX-induced growth inhibition. p53-null H1299 cells were also more resistant to MTX-induced growth inhibition (Fig. 4C), confirming the essential role of p53 in MTX-induced cytoxicity.

### 3.5. MTX increased E-cadherin through downregulation of HDAC/EZH2

MDM2 has been reported to recruit HDAC1 and remove acetyl groups from p53 to promote its degradation, leading to the

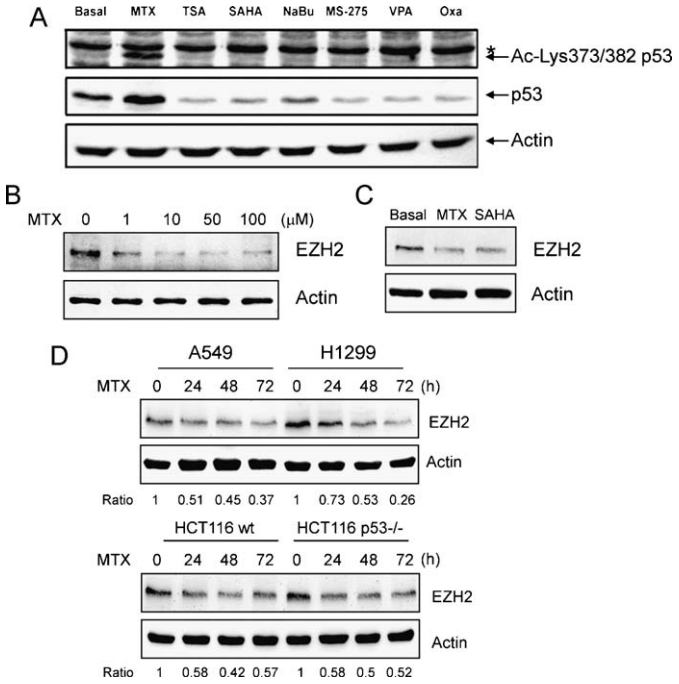


**Fig. 5.** Effect of MTX on EZH2 expression. (A) A549 cells were treated with 50 μM MTX, 1 μM TSA, 5 μM SAHA, 1 mM sodium butyrate (NaBu), 10 μM MS-275, 5 mM valproic acid (VPA), 10 μM oxaflatin (Oxa) for 24 h. Total cell lysates were immunoblotted with anti-p53 (DO-1), anti-acetyl-p53 (Lys373/382) or actin antibodies. *Non-specific band. (B) A549 cells were exposed to 1, 10, 50, 100 μM MTX for 48 h, and whole cell lysates were collected and blotted with anti-EZH2 antibody. (C) A549 cells were treated with 50 μM MTX and 5 μM SAHA for 48 h and whole cell lysates were subjected with immunoblotting with antibody against EZH2. (D) A549, H1299, HCT116 wt and HCT116 p53−/− cells were treated with 50 μM MTX as indicated time, and whole cell lysates were immunoblotted with indicated antibodies.

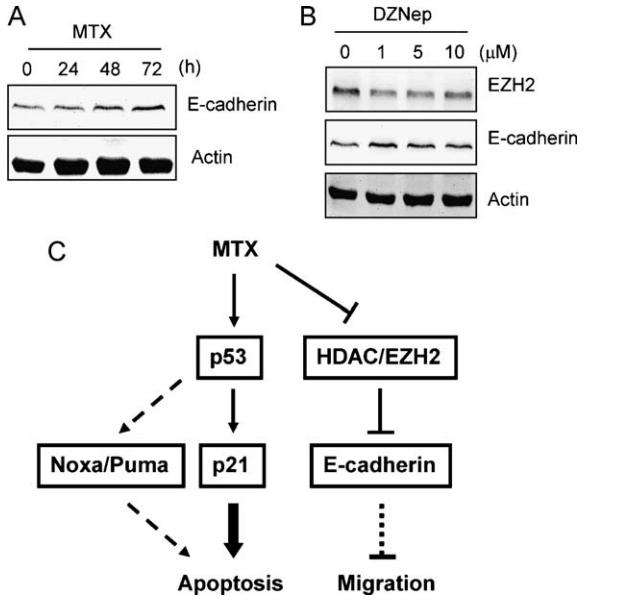


**Fig. 6.** Effect of MTX on E-cadherin expression. (A) A549 cells were treated with 50 μM MTX as indicated time, and whole cell lysates were immunoblotted with indicated antibodies. (B) A549 and H1299 cells were subjected to 1, 5 and 10 μM DZNep for 72 h, and whole cell lysates were immunoblotted with indicated antibodies. (C) The working model for the anticancer effects of MTX.

inhibition of p53 transcriptional activity [25,26]. Our recent study demonstrates that MTX inhibits HDAC activity [27]. Whether HDAC inhibition leads to p53 acetylation was examined. As shown in Fig. 5A, HDAC inhibitors did not induce p53 acetylation and expression, suggesting that inhibition of HDAC is dispensable for MTX to induce p53 expression.

Inhibition of HDAC has been reported to lead to the degradation of EZH2 [28]. We also found that MTX inhibited EZH2 expression dose-dependently (Fig. 5B), as did by HDAC inhibitor SAHA (Fig. 5C). E-cadherin was reported to be transcriptional silenced by EZH2-mediated trimethlyation of histone H3 lysine 27 [20]. Since EZH2 was decreased in response to MTX in both p53-wildtype (A549) and p53-deficient (H1299) cells (Fig. 5D), E-cadherin protein level was further examined. MTX increased E-cadherin expression time-dependently in A549 cell (Fig. 6A), as did by the EZH2 inhibitor DZNep (Fig. 6B). Therefore, MTX increased E-cadherin expression through downregulation of HDAC/EZH2.

## 4. Discussion

NSCLC is the most prevalent type of lung cancer. Cisplatin-based chemotherapy has been extensively used for the past two decades and MTX is one of the most frequently used agents in combination with cisplatin [29]. However, the molecular targets of MTX against NSCLC have not been investigated. In this study, we showed that MTX inhibits NSCLC A549 cell growth in culture and xenograft model. The anticancer mechanism of MTX acts through initiation of p53-dependent apoptosis and restoration of E-cadherin expression by inhibiting HDAC/EZH2.

Acetylation and deacetylation can modulate protein–protein interaction, protein stability and subcellular localization [30]. p53 is the first non-histone protein found to be acetylated at lysine residues [8]. Our results showed that MTX but not HDAC inhibitors induced acetylation of p53, indicating that inhibition of HDAC by MTX was dispensable for p53 acetylation. The acetylation of p53 was correlated with its nuclear accumulation and stability. The lysine residues acetylated are also the sites for ubiquitination. Acetylation of p53 can prevent its ubiquitination and the subsequent degradation by proteasome [31]. Phosphorylation of p53 can increase its stabilization as well. Our results show that MTX induced phosphorylation of p53 at Ser15, which appears to be prerequisite for the subsequent post-translational modifications [32]. However, p53 can also be activated regardless of its phosphorylation [33,34]. Acetylation of p53 during stress response is sufficient for abrogating MDM2-mediated repression in the absence of phosphorylation [35]. The relationship between phoshorylation and acetylation of p53 in response to MTX warrants further investigations.

Sequence-specific DNA binding of p53 is a prerequisite for the transactivation of target genes. The binding affinity on specific p53 response elements (p53REs) differs widely. Generally, binding to high-affinity p53REs tends to upregulate growth arrest-related genes, whereas binding to low-affinity p53REs is associated with proapoptotic genes [36]. Site-specific acetylation dictates the target preferences of p53 and exerts unique outcomes. For example, acetylation at Lys320 only allows activation of genes containing high-affinity p53 binding sites, leading to cell cycle arrest. In contrast, acetylation at Lys373 enhances its interaction with low-affinity p53 binding sites, leading to apoptosis [37]. MTX induced p53 acetylation at Lys373/382, and apoptosis was indeed observed after MTX treatment. Although MTX induced expression of p21 probably through high-affinity p53 binding sites, we could not exclude the possibility that acetylation of the other sites such as Lys320 might occur. However, cell cycle arrest was not seen after MTX treatment. It is probable that Lys373/382 acetylation is sufficient to induce p21 expression. The result that depsipeptide induces p21 expression through acetylation of p53 at Lys373/382 but not Lys320 supports this notion [38].

p21 is a member of cyclin-dependent kinase (CDK) inhibitors (CKI), which negatively modulates cell cycle by inhibiting cyclin–CDK complex [39]. MTX induced apoptosis but not cell cycle arrest, and apoptosis was attenuated in p21 deficient cells. Although p21 is required for p53-dependent G1 and G2/M arrest [40,41], elevating sensitivity to apoptotic stimuli by increasing Bax or antagonizing Bcl-2 expression has been reported [42–44]. Moreover, cell viability was not fully recovered in p21 null cells, indicating that other p53-dependent signaling might collaboratively contribute to MTX-induced apoptosis. p53 can mediate apoptosis through intrinsic (such as Bax, Noxa, and Puma) and extrinsic (such as Fas and DR5 receptor) pathways [45]. MTX-induced DR5, Puma and Noxa expression might contribute to p53-dependent apoptosis.

Although E-cadherin expression is reduced in many NSCLC patients [46], NSCLC expressing E-cadherin may carry a better prognosis than E-cadherin-negative tumors [47]. Restoring E-cadherin by HDAC inhibitors or by ecotopic expression can increase the sensitivity of epidermal growth factor receptor (EGFR) inhibitors to lung cancer cells [48]. Thus, E-cadherin expression induced by MTX might provide a therapeutic consideration in NSCLC. There are several epigenetic mechanisms suppressing E-cadherin expression. For example, it is silenced by DNA hypermethylation in human carcinomas [49,50]. In addition, recruitment of transcriptional corepressors or chromatin-remodeling protein to E-cadherin promoter suppresses its expression [51–53]. EZH2 has been reported to downregulate E-cadherin through trimethylation of histone H3 lysine27 [20]. In this study, inhibition of EZH2 by DZNep increased E-cadherin expression. MTX induced E-cadherin expression as well and correlated with its downregulation of EZH2, suggesting that MTX could increase E-cadherin expression via epigenetic downregulation of EZH2. Consistent with a previous report that HDAC inhibitors deplete EZH2 [28], the suppression of EZH2 by MTX might be resulted from its inhibition on HDAC activity [27].

In sum, we show that MTX exhibits anti-tumor activity against NSCLC A549 cells *in vitro* and *in vivo*. Post-translational modifications including acetylation at Lys373/382 and phosphorylation at Ser15 stabilize p53 protein expression. MTX-induced apoptosis is dependent on p53 and, partially, p21. Furthermore, MTX inhibits both EZH2 expression and HDAC activity to induce E-cadherin expression, which might reduce cell migration (Fig. 6D). Our report provides a molecular mechanism for MTX to suppress NSCLC.

## Acknowledgment

This work was supported by a research grant from National Science Council of Taiwan (NSC 97-2320-B002-033-MY3).

## References

[1] DeCicco KL, Tanaka T, Andreola F, De Luca LM. The effect of thalidomide on non-small cell lung cancer (NSCLC) cell lines: possible involvement in the PPARgamma pathway. Carcinogenesis 2004;25:1805–12.
[2] Yang P, Allen MS, Aubry MC, Wampfler JA, Marks RS, Edell ES, et al. Clinical features of 5628 primary lung cancer patients: experience at Mayo Clinic from 1997 to 2003. Chest 2005;128:452–62.
[3] Manegold C. Chemotherapy for advanced non-small cell lung cancer: standards. Lung Cancer (Amsterdam Netherlands) 2001;34(Suppl. 2):S165–70.
[4] Haupt Y, Maya R, Kazaz A, Oren M. Mdm2 promotes the rapid degradation of p53. Nature 1997;387:296–9.
[5] Vousden KH, Lu X. Live or let die: the cell's response to p53. Nat Rev Cancer 2002;2:594–604.
[6] Bode AM, Dong Z. Post-translational modification of p53 in tumorigenesis. Nat Rev Cancer 2004;4:793–805.
[7] Ito A, Lai CH, Zhao X, Saito S, Hamilton MH, Appella E, et al. p300/CBP-mediated p53 acetylation is commonly induced by p53-activating agents and inhibited by MDM2. EMBO J 2001;20:1331–40.
[8] Gu W, Shi XL, Roeder RG. Synergistic activation of transcription by CBP and p53. Nature 1997;387:819–23.
[9] Kleer CG, Cao Q, Varambally S, Shen R, Ota I, Tomlins SA, et al. EZH2 is a marker of aggressive breast cancer and promotes neoplastic transformation of breast epithelial cells. Proc Natl Acad Sci USA 2003;100:11606–11.
[10] Varambally S, Dhanasekaran SM, Zhou M, Barrette TR, Kumar-Sinha C, Sanda MG, et al. The polycomb group protein EZH2 is involved in progression of prostate cancer. Nature 2002;419:624–9.
[11] Raaphorst FM, Meijer CJ, Fieret E, Blokzijl T, Mommers E, Buerger H, et al. Poorly differentiated breast carcinoma is associated with increased expression of the human polycomb group EZH2 gene. Neoplasia 2003;5:481–8.
[12] Breuer RH, Snijders PJ, Smit EF, Sutedja TG, Sewalt RG, Otte AP, et al. Increased expression of the EZH2 polycomb group gene in BMI-1-positive neoplastic cells during bronchial carcinogenesis. Neoplasia 2004;6:736–43.
[13] van der Vlag J, Otte AP. Transcriptional repression mediated by the human polycomb-group protein EED involves histone deacetylation. Nat Genet 1999;23:474–8.
[14] Bolden JE, Peart MJ, Johnstone RW. Anticancer activities of histone deacetylase inhibitors. Nat Rev Drug Discov 2006;5:769–84.
[15] Croonquist PA, Van Ness B. The polycomb group protein enhancer of zeste homolog 2 (EZH 2) is an oncogene that influences myeloma cell growth and the mutant ras phenotype. Oncogene 2005;24:6269–80.
[16] Tan J, Yang X, Zhuang L, Jiang X, Chen W, Lee PL, et al. Pharmacologic disruption of polycomb-repressive complex 2-mediated gene repression selectively induces apoptosis in cancer cells. Genes Dev 2007;21:1050–63.
[17] Damsky CH, Richa J, Solter D, Knudsen K, Buck CA. Identification and purification of a cell surface glycoprotein mediating intercellular adhesion in embryonic and adult tissue. Cell 1983;34:455–66.
[18] Moll R, Mitze M, Frixen UH, Birchmeier W. Differential loss of E-cadherin expression in infiltrating ductal and lobular breast carcinomas. Am J Pathol 1993;143:1731–42.
[19] Oka H, Shiozaki H, Kobayashi K, Inoue M, Tahara H, Kobayashi T, et al. Expression of E-cadherin cell adhesion molecules in human breast cancer tissues and its relationship to metastasis. Cancer Res 1993;53:1696–701.
[20] Cao Q, Yu J, Dhanasekaran SM, Kim JH, Mani RS, Tomlins SA, et al. Repression of E-cadherin by the polycomb group protein EZH2 in cancer. Oncogene 2008;27:7274–84.
[21] Chao YL, Shepard CR, Wells A. Breast carcinoma cells re-express E-cadherin during mesenchymal to epithelial reverting transition. Mol Cancer 2010;9:179.
[22] Olsen EA. The pharmacology of methotrexate. J Am Acad Dermatol 1991;25:306–18.
[23] Lorico A, Toffoli G, Boiocchi M, Erba E, Broggini M, Rappa G, et al. Accumulation of DNA strand breaks in cells exposed to methotrexate or N10-propargyl-5,8-dideazafolic acid. Cancer Res 1988;48:2036–41.
[24] Villunger A, Michalak EM, Coultas L, Mullauer F, Bock G, Ausserlechner MJ, et al. p53- and drug-induced apoptotic responses mediated by BH3-only proteins puma and noxa. Science 2003;302:1036–8.
[25] Juan LJ, Shia WJ, Chen MH, Yang WM, Seto E, Lin YS, et al. Histone deacetylases specifically down-regulate p53-dependent gene activation. J Biol Chem 2000;275:20436–43.
[26] Ito A, Kawaguchi Y, Lai CH, Kovacs JJ, Higashimoto Y, Appella E, et al. MDM2-HDAC1-mediated deacetylation of p53 is required for its degradation. EMBO J 2002;21:6236–45.
[27] Yang PM, Lin JH, Huang WY, Lin YC, Yeh SH, Chen CC. Inhibition of histone deacetylase activity is a novel function of antifolate drug methotrexate. Biochem Biophys Res Commun 2010;391:1396–9.
[28] Fiskus W, Pranpat M, Balasis M, Herger B, Rao R, Chinnaiyan A, et al. Histone deacetylase inhibitors deplete enhancer of zeste 2 and associated polycomb repressive complex 2 proteins in human acute leukemia cells. Mol Cancer Ther 2006;5:3096–104.
[29] Grossi F, Aita M, Follador A, Defferrari C, Brianti A, Sinaccio G, et al. Sequential, alternating, and maintenance/consolidation chemotherapy in advanced non-small cell lung cancer: a review of the literature. Oncologist 2007;12:451–64.
[30] Glozak MA, Seto E. Histone deacetylases and cancer. Oncogene 2007;26:5420–32.
[31] Li M, Luo J, Brooks CL, Gu W. Acetylation of p53 inhibits its ubiquitination by Mdm2. J Biol Chem 2002;277:50607–11.
[32] Appella E, Anderson CW. Post-translational modifications and activation of p53 by genotoxic stresses. Eur J Biochem 2001;268:2764–72.
[33] Blattner C, Tobiasch E, Litfen M, Rahmsdorf HJ, Herrlich P. DNA damage induced p53 stabilization: no indication for an involvement of p53 phosphorylation. Oncogene 1999;18:1723–32.
[34] Thomson T, Tovar C, Yang H, Carvajal D, Vu BT, Xu Q, et al. Phosphorylation of p53 on key serines is dispensable for transcriptional activation and apoptosis. J Biol Chem 2004;279:53015–22.
[35] Tang Y, Zhao W, Chen Y, Zhao Y, Gu W. Acetylation is indispensable for p53 activation. Cell 2008;133:612–26.
[36] Inga A, Storici F, Darden TA, Resnick MA. Differential transactivation by the p53 transcription factor is highly dependent on p53 level and promoter target sequence. Mol Cell Biol 2002;22:8612–25.
[37] Knights CD, Catania J, Di Giovanni S, Muratoglu S, Perez R, Swartzbeck A, et al. Distinct p53 acetylation cassettes differentially influence gene-expression patterns and cell fate. J Cell Biol 2006;173:533–44.
[38] Zhao Y, Lu S, Wu L, Chai G, Wang H, Chen Y, et al. Acetylation of p53 at lysine 373/382 by the histone deacetylase inhibitor depsipeptide induces expression of p21(Waf1/Cip1). Mol Cell Biol 2006;26:2782–90.

[39] May P, May E. Twenty years of p53 research: structural and functional aspects of the p53 protein. Oncogene 1999;18:7621–36.
[40] Waldman T, Kinzler KW, Vogelstein B. p21 is necessary for the p53-mediated G1 arrest in human cancer cells. Cancer Res 1995;55:5187–90.
[41] Bunz F, Dutriaux A, Lengauer C, Waldman T, Zhou S, Brown JP, et al. Requirement for p53 and p21 to sustain G2 arrest after DNA damage. Science 1998;282:1497–501.
[42] Lincet H, Poulain L, Remy JS, Deslandes E, Duigou F, Gauduchon P, et al. The p21(cip1/waf1) cyclin-dependent kinase inhibitor enhances the cytotoxic effect of cisplatin in human ovarian carcinoma cells. Cancer Lett 2000;161: 17–26.
[43] Qiao L, McKinstry R, Gupta S, Gilfor D, Windle JJ, Hylemon PB, et al. Cyclin kinase inhibitor p21 potentiates bile acid-induced apoptosis in hepatocytes that is dependent on p53. Hepatology 2002;36:39–48.
[44] Kang KH, Kim WH, Choi KH. p21 promotes ceramide-induced apoptosis and antagonizes the antideath effect of Bcl-2 in human hepatocarcinoma cells. Exp Cell Res 1999;253:403–12.
[45] Harris SL, Levine AJ. The p53 pathway: positive and negative feedback loops. Oncogene 2005;24:2899–908.
[46] Fei Q, Zhang H, Chen X, Wang JC, Zhang R, Xu W, et al. Defected expression of E-cadherin in non-small cell lung cancer. Lung Cancer (Amsterdam Netherlands) 2002;37:147–52.
[47] Bremnes RM, Veve R, Hirsch FR, Franklin WA. The E-cadherin cell–cell adhesion complex and lung cancer invasion, metastasis, and prognosis. Lung Cancer (Amsterdam Netherlands) 2002;36:115–24.
[48] Witta SE, Gemmill RM, Hirsch FR, Coldren CD, Hedman K, Ravdel L, et al. Restoring E-cadherin expression increases sensitivity to epidermal growth factor receptor inhibitors in lung cancer cell lines. Cancer Res 2006;66:944–50.
[49] Yoshiura K, Kanai Y, Ochiai A, Shimoyama Y, Sugimura T, Hirohashi S. Silencing of the E-cadherin invasion-suppressor gene by CpG methylation in human carcinomas. Proc Natl Acad Sci USA 1995;92:7416–9.
[50] Graff JR, Herman JG, Lapidus RG, Chopra H, Xu R, Jarrard DF, et al. E-cadherin expression is silenced by DNA hypermethylation in human breast and prostate carcinomas. Cancer Res 1995;55:5195–9.
[51] Lin T, Ponn A, Hu X, Law BK, Lu J. Requirement of the histone demethylase LSD1 in Snai1-mediated transcriptional repression during epithelial-mesenchymal transition. Oncogene 2010.
[52] Peinado H, Ballestar E, Esteller M, Cano A. Snail mediates E-cadherin repression by the recruitment of the Sin3A/histone deacetylase 1 (HDAC1)/HDAC2 complex. Mol Cell Biol 2004;24:306–19.
[53] Sanchez-Tillo E, Lazaro A, Torrent R, Cuatrecasas M, Vaquero EC, Castells A, et al. ZEB1 represses E-cadherin and induces an EMT by recruiting the SWI/SNF chromatin-remodeling protein BRG1. Oncogene 2010;29:3490–500.